Prediction of Hildebrand Solubility Parameters of Acrylate and Methacrylate Monomers and Their Mixtures by Molecular Simulation

John L. Lewin,[1,2,3] Katie A. Maerzke,[1,2] Nathan E. Schultz,[4] Richard B. Ross,[4] J. Ilja Siepmann[1,2]

[1]*Department of Chemistry, University of Minnesota, 207 Pleasant St. SE, Minneapolis, Minnesota 55453*
[2]*Departments of Chemistry and of Chemical Engineering and Materials Science, University of Minnesota, 207 Pleasant Street SE, Minneapolis, Minnesota 55455*
[3]*Department of Chemistry, Augsburg College, 2211 Riverside Avenue, Minneapolis, Minnesota 55454*
[4]*Corporate Research Materials Laboratory, 201-2E-23, 3M Company, St., Paul, Minnesota 55144*

Received 16 April 2009; accepted 2 August 2009
DOI 10.1002/app.31232
Published online 13 November 2009 in Wiley InterScience (www.interscience.wiley.com).

ABSTRACT: Hildebrand solubility parameters are predicted from molecular simulations using the transferable potentials for phase equilibrium-united atom (TraPPE-UA) and Dreiding force fields for the *n*-alkyl acrylate and methacrylate esters ($n \leq 10$), as well as the 2-ethylhexyl acrylate, 2-hydroxyethyl acrylate, isooctyl esters of acrylic acid, and the 2-hydroxyethyl ester of methacrylic acid. The TraPPE-UA force field yields very accurate solubility parameters (with a mean unsigned percent error of 2% or 0.2 Hildebrand units), whereas the Dreiding force field overpredicts the solubility parameter in every case examined. Correlations based on the normal boiling point or the refractive index do not yield satisfactory results for this monomer set with the former overestimating the magnitude and the latter yielding the incorrect sign for the decrease in the solubility parameter with chain length. Simulations with the TraPPE-UA force field yield solubility parameters for binary mixtures of methyl methacrylate with 2-ethylhexyl or isooctyl acrylate, which are very well described by a linear interpolation using the pure compound cohesive energies and molar volumes, whereas those for mixtures with 2-hydroxyethyl acrylate or methacrylate small positive deviations due to structural microheterogeneity. © 2009 Wiley Periodicals, Inc. J Appl Polym Sci 116: 1–9, 2010

Key words: solubility parameter; acrylates; methacrylates; Monte Carlo simulations

INTRODUCTION

The solubility parameter, δ, is widely used as a convenient means of predicting miscibility of compounds in a variety of applications, ranging from polymer blending[1,2] to dye sorption in polymers.[3] The concept was first introduced by Hildebrand and Scott[4] and is defined as the square root of the cohesive energy density (CED) [4–10]

$$\delta = \sqrt{\frac{\Delta E}{V_{\mathrm{m}}}} \tag{1}$$

where ΔE is the molar energy difference between a molecule in the vapor phase (assuming ideality) and one in the liquid phase, and V_m is the molar volume. Along the vapor–liquid coexistence line, it can be expressed as a function of the enthalpy of vaporization

$$\delta = \sqrt{\frac{\Delta H_{\mathrm{vap}} - RT}{V_{\mathrm{m}}}} \tag{2}$$

which provides the most reliable experimental route for the determination of the solubility parameter. The solubility parameter idea was expanded by Hansen to represent the geometric mean of additional parameters specific to dispersion (δ_{d}), polarizability/electrostatic (δ_p), and H-bonding interactions (δ_h), in the form

$$\delta_t^2 = \delta_d^2 + \delta_p^2 + \delta_h^2 \tag{3}$$

where δ_t is the "total" solubility parameter and is equivalent to the Hildebrand solubility parameter.[7,10–13] Because the heat of vaporization of a polymer cannot be measured experimentally, it is a common practice to use the corresponding value of the solubility parameter for its monomers as a substitute.

Additional Supporting Information may be found in the online version of this article.

Correspondence to: J. Ilja Siepmann (siepmann@umn.edu)

Contract grant sponsor: National Science Foundation; contract grant number: CBET-756641.
Contract grant sponsor: 3M Company.
Contract grant sponsor: Minnesota Supercomputing Institute.

Given the technological importance of the Hildebrand and Hansen solubility parameters for selecting solvents and designing polymer blends, there exist a number of compilations of solubility parameters for industrially relevant chemicals and materials.[5,6,9,13,14] Because heats of vaporization for polymers cannot be measured, the solubility tabulated in handbooks sometimes do not reflect direct experimental measurements but instead are based on group-additive or other approximate methods. Often a molecule of interest will have no reported value for its solubility parameter, predicted or experimental. In such a case, it would be very beneficial to be able to predict or calculate a molecule's solubility parameter with a technique more accurate than a group-additive scheme. Particle-based simulations with accurate force fields offer a promising alternative. This strategy has been pursued with success by Belmares et al.,[15] Aminabhavi and co-workers [16–18] and this research group[19,20] for a large set of diverse small molecules (solvents and monomers) and polymers with known solubility parameter values. The current work extends previous work into an area where solubility parameter data are scarce: the *n*-alkyl acrylate and methacrylate monomer series, together with other esters of branched chain and polar functionalities. Here, solubility parameters for the C1 to C10 *n*-alkyl acrylates and methacrylates and for acrylates with branched alkyl or 2-hydroxyethyl side chains are computed using Monte Carlo (MC) simulations and compared with experimental values (where available) and correlations. A particle-based MC simulation uses a sequence of stochastic moves to construct a trajectory of the system of interest that is subject to a set of thermodynamic constraints and where the interactions between the particles are described by a force field (or potential energy function).[21,22]

SIMULATION METHODOLOGY

Force fields

The transferable potentials for phase equilibria (TraPPE) force field in its united atom (UA) representation [23–27] was used for all *n*-alkyl acrylate and methacrylate monomers C1-C10, as well as for 2-hydroxyethyl acrylate (HEA), 2-hydroxy methacrylate (HEMA), 6-methylheptyl acrylate (often referred to as isooctyl acrylate, IOA), and 2-ethylhexyl acrylate (EHA). The TraPPE force field describes nonbonded interactions with Lennard-Jones (LJ) and Coulomb potentials. All molecules were treated as semiflexible to the extent possible: bond lengths are rigid, whereas bending angles are described by harmonic potentials, and torsional angles are described by cosine series potentials. For HEA and HEMA the alcohol hydrogen atom is represented only by a charge site. Full details of the TraPPE-UA acrylate model are given in the original reference.[27] Here, it should be noted that only the vapor–liquid coexistence curves of methyl acrylate and methyl methacrylate (MMA) were used in the parameterization of the TraPPE-UA acrylate model, i.e., the solubility parameters for these two compounds are indirectly (via the heat of vaporization and the saturated liquid density) considered in the parameterization, whereas the solubility parameters computed for all other compounds are predictions.

For comparison with the data computed for the TraPPE-UA force field, solubility parameters calculated using the molecular dynamics CED method developed by Belmares et al.[15] are also included. The CED method uses the Dreiding force field and charges computed from an electrostatic potential constructed at the HF/6-31G(d,p) level of electronic structure theory.[28] To our knowledge, neither acrylates nor methacrylates were considered in the parameterization of the Dreiding force field.

Simulation details

Solubility parameters at 298.15 K and 0.1 MPa were computed using MC simulations in the isobaric-isothermal (*NPT*) ensemble according to the equation[19,20]

$$\delta = \left\langle \sqrt{\frac{U_{\mathrm{iso}} - U_{\mathrm{liq}}}{V_{\mathrm{m}}}} \right\rangle_{\mathrm{NPT}} \tag{4}$$

where δ is the Hildebrand (total) solubility parameter, U_{iso} is the molar potential energy of an isolated molecule (computed separately from the bulk liquid), U_{liq} is the total molar potential energy of the bulk liquid phase, and V_m is the molar volume of the liquid phase. The SI units of δ are $\mathrm{MPa}^{1/2}$, but δ is commonly reported also in (Hildebrand) units of $(\mathrm{cal/cm}^3)^{1/2}$; the conversion between the two is a factor of $\sqrt{4.184}$.[5,7,10,13]

For all simulations, the system size consisted of 301 molecules in a two-box set-up (300 liquid-phase and 1-gas-phase molecules). A spherical potential truncation of $r_{\mathrm{cut}} = 14$ Å was used for LJ interactions, with analytic tail corrections applied.[21,22] All electrostatic interactions were computed by Ewald summation with a real space cutoff of 14 Å (r_{cut}) and the convergence parameter κ set to $3.2/r_{\mathrm{cut}}$.[21,22] Unlike LJ interaction, parameters were determined according to Lorentz-Berthelot combining rules.[29] These are the standard long-range interaction treatments and combining rules for the TraPPE-UA force field.

All systems were equilibrated for at least 250,000 MC cycles, where one cycle is made up of N moves, N being the number of molecules. In addition to the usual MC trial moves of center-of-mass translations and rotations, coupled–decoupled configurational-bias MC[24,30,31] moves (20% of trial moves) were used to allow the system to reach thermal equilibrium, whereas volume exchanges with an external pressure bath equilibrated the density. After the equilibration period, production runs of at least 300,000 MC cycles, divided into five blocks, were performed and data collected. Statistical uncertainties are estimated from the block averages and are reported as the standard error of the mean.

Mixtures

A selected number of mixtures were also investigated using the TraPPE-UA force field. These were chosen based on similar or dissimilar solubility parameters of the components, as well as potential industrial relevance, to ascertain whether the mixture solubility parameter can be well described by a linear interpolation of the pure compound solubility parameters or by using linear interpolations of the pure compound data on the right-hand side of eq. (4). Four types of mixtures (MMA/HEA, MMA/HEMA, MMA/EHA, and MMA/IOA) were simulated with the same method described above using 300 total liquid-phase molecules at five different molfractions. To compute the mixture solubility parameter via eq. (4), U_{liq} and V_{m} are taken directly from the simulation of the specific mixture, and the value of U_{iso} for the mixture is obtained by the sum of each mixture component's U_{iso} multiplied by its molfraction (i.e., $U_{\mathrm{iso}} = x_A U_{\mathrm{iso}}^A + x_B U_{\mathrm{iso}}^B$).

Experimental data and correlations

Experimentally determined solubility parameters were assembled for comparison with those computed in this work and are listed in the Supporting Information. These can be found in handbooks and sometimes in the primary literature. However, the term "experimental" is used advisedly; while some portion of a solubility parameter's value, such as ΔH_{vap}, may be experimentally determined, other components, such at the molar volume at 298.15 K, may originate from group-additive methods. Many compilations state this fact plainly although some do not, nor is it always clear which part is experimentally determined.[6,13,14] Moreover, the experimental components are not always measured in the same way, giving rise to multiple dissimilar values.[13,15] For the n-alkyl acrylates and methacrylates, and esters of these monomers in general, this problem is compounded by the almost complete lack of solubility parameter values, or even much physical property data, for linear chains longer than n-butyl (C4).

For n-alkyl acrylate and methacrylate esters, correlations based on the normal boiling point or the refractive index can be used to estimate the solubility parameter. The normal boiling points (1 atm) of the n-alkyl acrylates and the n-alkyl methacrylates can be described according to the experimentally derived equation[32]

$$T_{\mathrm{b}} = \sqrt{ax + b} \tag{5}$$

where T_{b} is the normal boiling point in Kelvin and x is the total number of carbon atoms in the molecule; the values of the parameters for the acrylates (methacrylates) are a = 18,700 (18,400) and b = 44,000 (42,000).[32] These relationships yield good agreement with other available experimental boiling points. These and available boiling points then can be used to estimate ΔH_{vap} with the Hildebrand rule[4,5,7,8]

$$\Delta H_{\mathrm{vap}} = -12,340 + 99.2(T_{\mathrm{b}}) + 0.084(T_{\mathrm{b}}{}^2) \tag{6}$$

where ΔH_{vap} is given in Joules per mole and T_{b} is in Kelvin. Enthalpies of vaporization so computed were used to determine Hildebrand solubility parameters using eq. (2), where molar volumes were determined from experimental densities at 20°C (293 K). Experimentally derived molar volumes are listed in the Supporting Information. It is worth noting here that experimental densities are often reported at 20°C, such as the majority of those in the CRC Handbook.[33] Moreover, as with other "experimental" solubility parameter data, it is not clear whether the molar volume used in computing these values is properly determined at 25°C (since solubility parameters are reported at this temperature), or if they are in fact from densities at 20°C. Although the effect on the solubility parameter will be small, this issue is merely one of the many to consider when assessing the relative accuracy or inaccuracy of a solubility parameter's purportedly experimental value.

Another popular approach is to estimate the solubility parameters from measured refractive index values, which are often available for the acrylate and methacrylate esters. These correlations usually do not include a dependence on the molar volume and, hence, predict an increase in the solubility parameter with increasing refractive index; one commonly used correlation for the Hansen δ_{d} parameter (in $\mathrm{MPa}^{1/2}$) is

$$\delta_{\mathrm{d}} = 9.55 n_D - 5.55 \tag{7}$$

where n_{D} is the refractive index.[5,7,34] Another equation purporting to predict the total Hildebrand

solubility parameter with the refractive index was fit to the Lorentz-Lorenz function (as are many similar methods) and is given by

$$\delta = \sqrt{304.5\left(\frac{n_D^2 - 1}{n_D^2 + 2}\right)} \quad (8)$$

where δ is the Hildebrand solubility parameter in $(cal/cm^3)^{1/2}$ and 304.5 is an empirically determined constant.[35] A table with refractive indices and the corresponding δ values calculated from eq. (8) is provided in the Supporting Information.

RESULTS AND DISCUSSION

Comparison with the literature data

Figure 1 shows a comparison of the Hildebrand (total) solubility parameters for the *n*-alkyl, 2-ethylhexyl, and 2-hydroxyethyl acrylates and methacrylates computed using MC simulations with the TraPPE-UA force field with those computed to the CED method using the Dreiding force field,[15] together with solubility parameters taken from the literature (based on the experimental data[6,8,9,13,36,37] or group additivity methods[14]). Numerical values of the simulation data (with statistical uncertainties for the TraPPE-UA data) are listed in the Supporting Information. In general, the TraPPE-UA force field does very well, yielding a mean unsigned percent error (MUPE) of 1.7 for the acrylates and 2.2 for the methacrylates, versus the Dreiding force field that gives MUPEs of 12 and 10 for the acrylates and methacrylates, respectively. For six of the seven acrylates and methacrylates for which multiple literature values could be found, the TraPPE-UA prediction falls within the range of the literature data; the exception is EHA where the literature values appear somewhat small compared with those for the *n*-alkyl acrylates (with shorter side chains). Larger deviations between the TraPPE prediction and the single literature value are also observed for *n*-hexyl acrylate and *n*-propyl methacrylate. For the former, the literature value is from Hoy[9] and is of questionable accuracy because it does not follow a regular trend with the data for other *n*-alkyl acrylate from the same source (C1: 9.38; C2: 8.81; C4: 8.63; C6: 8.69). For *n*-propyl methacrylate, the single literature value from Hansen[13] falls significantly above the average literature values for the ethyl and *n*-butyl methacrylates (see Supporting Information). In contrast to the satisfactory predictions obtained with the TraPPE-UA force field, the Dreiding results greatly overpredict the solubility parameter value in every case and the deviations are largest for acrylates with short side chains (i.e., those with the largest value of the solubility parameter).

Dependence on side-chain length and comparison with correlations

The MC simulations for the TraPPE-UA force field yield a linear dependence of both the cohesive energy and the molar volume [see eq. (4)] with the side-chain length for the *n*-alkyl acrylates ($\Delta U(n)/[kJ/mol] = 4.298n + 26.31$ with $R^2 = 0.998$; $V(n)/[cm^3/mol] = 16.54n + 77.49$ with $R^2 = 0.999$) and methacrylates ($\Delta U(n)/[kJ/mol] = 4.186n + 30.02$ with $R^2 = 0.997$; $V(n)$ $[cm^3/mol] = 16.59n + 93.98$ with $R^2 = 0.999$). The similar coefficients (slopes) obtained for the acrylates and methacrylates indicate that fits of nearly the same quality can be obtained by using the same methylene increments for both homologous series. Here, it should be noted that the molar volumes predicted by the TraPPE-UA force field are in excellent agreement with the literature data[5,6,13,14,32,33,38–40] (with MUPEs of 1.0 and 1.2 for acrylates and methacrylates, respectively), whereas the Dreiding predictions are only of similar accuracy for shorter side chains with one to four carbon atoms but diverge with increasing side-chain length greater than five carbons (for numerical values, see Supporting Information). As a side note, this linear behavior of the cohesive energy will likely disappear when the length of the side chain is increased beyond the persistence length for alkyl chains because coiling allows the side chain to solvate itself, thus reducing the number of intermolecular contacts with other chains. Indeed, the vapor–liquid coexistence curves for linear and branched alkanes with more than 20 carbon atoms show significant deviations from the principle of corresponding states.[41]

Since the numerator and denominator in eq. (4) are both linear functions of side-chain length, the solubility parameter should converge to a limiting value with increasing side-chain length. The data presented in Figure 2 indicate that this is indeed the case for the TraPPE-UA predictions for the *n*-alkyl acrylates and methacrylates. The data for the Dreiding force field show considerably more scatter, but it should be noted that the CED method[15] is based on simulations much shorter than those used in this work.

Figure 2 also shows a comparison with two common correlation approaches for the solubility parameter that are either based on the normal boiling point and the Hildebrand rule [eqs. (5) and (6)] or on the refractive index [eq. (8)]. Neither of these correlations yields a satisfactory description of the side-chain length dependence of the solubility parameter. The boiling-point correlation is fairly accurate for

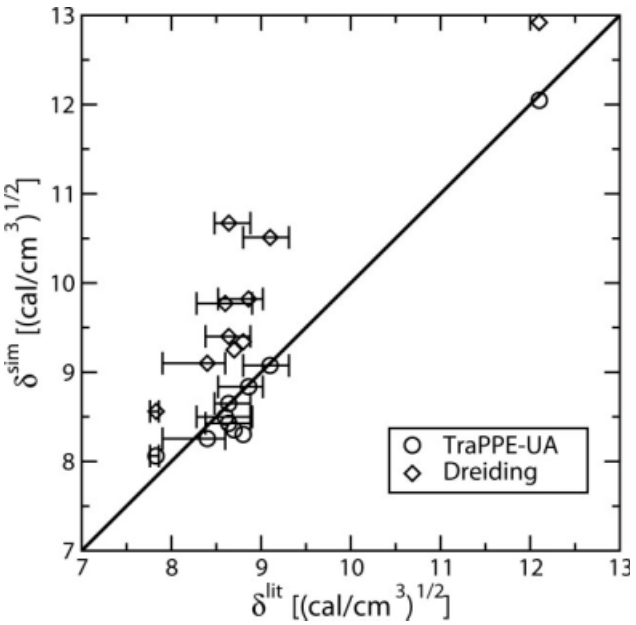

Figure 1 Scatter plot showing computed Hildebrand solubility parameters versus the literature data.[6,8,9,13,14,36,37] Data computed for the TraPPE-UA and Dreiding force fields are shown as circles and diamonds, respectively. The horizontal "error" bar indicates the range of literature data with the symbol being placed at the location of the unweighted average of the literature data.

short side chains (up to 4 carbon atoms), but overestimates the decrease in the Hildebrand solubility parameter for the acrylates and methacrylates with longer side chains. Because the boiling points for *n*-octyl acrylate and *n*-octyl methacrylate predicted by eq. (5) are in excellent agreement with the experimental data, it seems that the Hildebrand rule [eq. (6)] is responsible for the deviations observed for the larger acrylates. This does not come as a surprise because the Hildebrand rule (and also the principle of corresponding states) works best when applied to nearly spherical molecules where the interaction energy depends only on intermolecular distance and not orientation.[42]

For the *n*-alkyl esters of both the acrylates and methacrylates, the refractive indices increase with increasing chain length, and therefore the solubility parameters predicted by eq. (8) also increase accordingly, in contrast to experimental observation and the values predicted from simulation in this work, which decrease nonlinearly as a function of increasing chain length (see Fig. 2). It seems that the refractive index does not correctly reflect the larger incremental molar volume compared with the incremental cohesive energy. As an aside, one should note that eq. (8) yields solubility parameters of HEA and HEMA that are underpredicted by approximately 20% (see Supporting Information), i.e., the difference between an ethyl and a hydroxyethyl side chain is vastly underestimated. Although these and other correlative methods often represent an average over many different chemical functionalities, and the scarcity of physical property data can sometimes render such methods attractive, molecular simulation seems to hold greater promise with physically meaningful results.

Dispersive and polar contributions to the solubility parameter

Solubility parameters are often divided into three contributions [see eq. (3)] and Table I lists the individual contributions computed with the TraPPE-UA and Dreiding force fields and those found in Hansen's handbook.[13] Of course, there is no direct way to separate experimentally measured heats of vaporization (or molar volumes) into individual contributions, and thus a multitude of different estimation methods is used.[13] It should be noted that the TraPPE-UA force field does not contain any explicit H-bonding terms (i.e., the H-bonding is described through a balance of Coulombic and LJ interactions) and therefore the solubility parameter can only be divided into the dispersive (δ_d) and polar/electrostatic (δ_p) solubility parameters. The TraPPE-UA and Dreiding values for δ_d and δ_p decrease fairly

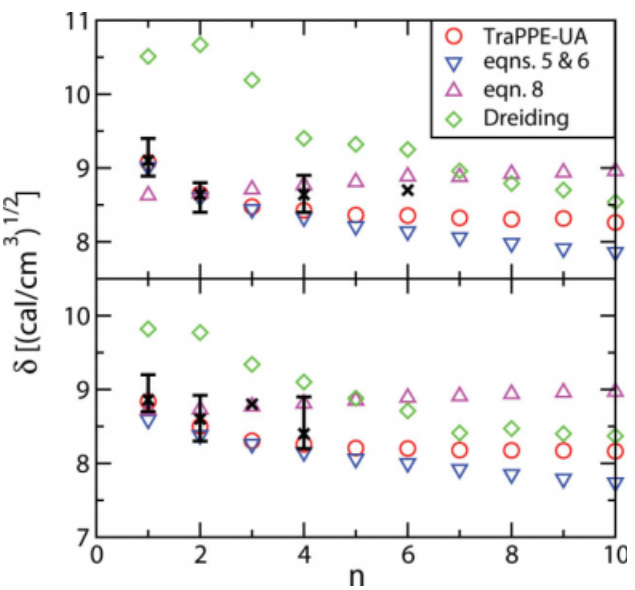

Figure 2 Side-chain length dependence of the Hildebrand solubility parameter for *n*-alkyl acrylates (top) and methacrylates (bottom). Red circles, green diamonds, blue down triangles, and magenta up triangles denote predictions based on the TraPPE-UA force field, the Dreiding force field, the boiling-point correlation [eqs. (5) and (6)[32]], and the refractive index correlation [eq. (8)[35]]. The vertical "error" bar and the cross indicate the range of the literature data.[6,8,9,13,14,36,37] [Color figure can be viewed in the online issue, which is available at www.interscience.wiley.com.]

TABLE I
Dispersive (δ_d), Polar (δ_p), and H-Bonding (δ_h) Solubility Parameters of Selected Acrylates and Methacrylates Computed With the TraPPE-UA and Dreiding Force Fields and Determined by Hansen[13] in Units of $(cal/cm^3)^{1/2}$

	TraPPE-UA		Dreiding			Hansen		
	δ_d	δ_p	δ_d	δ_p	δ_h	δ_d	δ_p	δ_h
Acrylate esters								
Methyl	8.79	2.71	8.31	6.53	0.00	7.48	3.28	4.60
Ethyl	8.53	2.15	8.51	6.17	0.00	7.58	3.47	2.69
n-Propyl	8.40	1.86	8.40	5.52	0.00			
n-Butyl	8.36	1.69	8.27	4.62	0.00	7.63	3.03	2.40
n-Decyl	8.24	1.14	8.00	3.25	0.00			
2-Ethylhexyl	8.11	1.22	7.85	3.33	0.00	7.24	2.30	1.66
2-Hydroxyethyl	8.76	8.49	8.30	9.03	3.81	7.82	6.45	6.55
Methacrylate esters								
Methyl	8.64	2.37	8.34	5.38	0.00	7.72	3.18	2.64
Ethyl	8.39	1.93	8.38	4.72	0.00	7.72	3.52	3.67
n-Propyl	8.27	1.69	8.23	4.34	0.00	7.58	3.08	3.23
n-Butyl	8.23	1.57	8.31	3.94	0.00	7.63	3.13	3.23

smoothly with increasing chain length for *n*-alkyl esters. This decrease in the δ_d values with increasing chain length is another interesting contrast to the increase predicted using refractive index data [see eq. (7)], i.e., the correlation also does not hold for δ_d alone. The values of δ_d computed for the TraPPE-UA force field are slightly larger (on average by approximately 3%) than those for the Dreiding force field which, in turn, are about 8% larger than those provided by Hansen.[13]

In contrast, the δ_p values differ significantly. The δ_p values determined with the Dreiding force field are nearly three times larger than those computed with TraPPE-UA and approximately 60% larger than the Hansen δ_p values, giving rise to the large overprediction of the total Hildebrand solubility parameters for the Dreiding force field (see Fig. 1), which are, within statistical uncertainties (for the simulations), the geometric means of the individual solubility parameters. The exception is HEA for which the Dreiding and TraPPE-UA δ_p are similar (see below). This large difference in the δ_p values is the result of the different partial atomic charge descriptions used by the two force fields: the TraPPE-UA acrylate model[27] places partial charges on only four atom centers and their value is independent of the length of the side chain, whereas the Dreiding model[15,28] places partial charges on every atom and the magnitude of the ester functional group is more polarized for longer side chains (see Supporting Information). Previously, it was already argued that the acrylate partial charges of the TraPPE-UA force field might be slightly too small in magnitude because the separation factor with alkanes is underestimated.[27] For the most polarized portion of the molecules, the carbonyl carbon, carbonyl oxygen, and the ester oxygen the Dreiding partial charges are larger by factors of about 2.5, 1.5, and 2, respectively, than those for the TraPPE-UA force field. Because the Dreiding force field significantly overestimates the Hildebrand (total) solubility parameters for the compounds of interest, it seems likely that its partial charges are too large in magnitude. To ascertain whether the CED predictions with the Dreiding force field could be improved by using a different charge model, partial charges were also computed from an electrostatic potential constructed at the B3LYP/6-31G** level of electronic structure theory.[43] Indeed the use of this level results in slightly reduced partial charges and the CED predictions for δ_p decrease to values of 5.88 and 4.83 for methyl acrylate and MMA, respectively, and concomitantly the Hildebrand solubility parameters for these compounds decrease by 3% and 4%, respectively, but remain too large compared with the literature averages by 12% and 7%, respectively.

HEA and HEMA are the only compounds studied here that contain both H-bond acceptors and donors. Hence, H-bonds cannot be present for pure phases of the other alkyl esters and the Dreiding force field yields δ_h values of zero for these compounds. In contrast, the Hansen δ_h values are non-zero for compounds that contain only acceptor or only donor sites. Because of H-bond formation, the TraPPE-UA force field predicts a large δ_p value for HEA (about four times larger than for ethyl acrylate). The Dreiding force field yields a similar δ_p value (as TraPPE-UA) for HEA and a δ_h value that is about a factor of 2.4 smaller than the δ_p value. In contrast, the Hansen δ_p and δ_h values are close in magnitude, and their geometric mean is about 9% smaller than that for the Dreiding force field and 7% larger than δ_p for the TraPPE-UA force field.

Mixtures

Molecular simulation can also be used to directly determine the Hildebrand solubility parameter for a

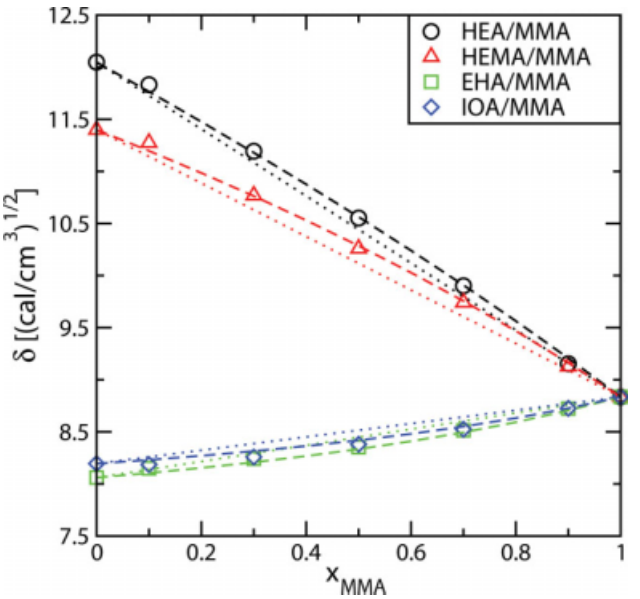

Figure 3 Composition dependence of the solubility parameter for four binary mixtures: HEA/MMA (black cirles and lines), HEMA/MMA (red triangles and lines), EHA/MMA (green squares and lines), and IOA/MMA (blue diamonds and lines). The symbols denote the results of explicit simulations with the TraPPE-UA force field for these binary mixtures. The dotted and dashed lines show a linear interpolation of the solubility parameters and an estimation based on eq. (4) using separate linear interpolations for the cohesive energy and molar volume. [Color figure can be viewed in the online issue, which is available at www.interscience.wiley.com.]

mixture. In principle, these mixture δ can also be determined from experimental measurements of the pure-component δ, and the excess heat and excess volume of mixing. However, to our knowledge, experimental data are not available for acrylate mixtures. When explicit data for a mixture are not available, the Hildebrand solubility parameter is often evaluated from a linear interpolation of the pure-component parameters. Figure 3 shows a comparison of the Hildebrand solubility parameters for four mixtures (HEA/MMA, HEMA/MMA, EHA/MMA, and IOA/MMA) as a function of composition computed directly from simulations against two linear interpolations: (i) a simple linear interpolation of the solubility parameter based on the molfraction (sometimes, the volume fraction is used for this interpolation, but the molar volumes of HEA, HEMA, and MMA are sufficiently close that the difference between molfraction and volume fraction interpolation would be very small), and (ii) an estimation that uses separate linear interpolations for the cohesive energy and the molar volume in eq. (4). Both interpolations use the pure-component properties obtained for the TraPPE-UA force field, so that the focus is on deviations caused by mixing. The data in Figure 3 indicate clearly that the interpolation using eq. (4) is significantly more accurate than the simple linear interpolation. The fact that the former works quite well implies that the relative values of the excess heat and volume of mixing are quite small for these mixtures.

The structural properties of these mixtures were also examined, and this discussion focuses on the 50/50 (molfraction) mixtures. To examine the microheterogeneity, the local molfraction enhancement (LMFE)[25,27] was determined as a function of center-of-mass distance from a chosen molecule. The local molfraction is the average number of molecules of a given type up to a distance r from the chosen molecule divided by the total number of molecules of any type, where the number of molecules of each type is determined from the center-of-mass number integral.[21,22] To obtain the local molfraction enhancement, the local molfraction is divided by the bulk mole fraction.[25] The data depicted in Figure 4 indicate a small LMFE for the 2-hydroxyethyl esters in the HEA/MMA and HEMA/MMA mixtures. Because the more polar esters have a slight tendency to aggregate, the likelihood to find an MMA molecule surrounded by a like species is also slightly enhanced. The reason for this aggregation is that the hydroxyl oxygen is a better acceptor site than the carbonyl and ester oxygen atoms of the acrylate moiety. This can be evaluated through an analysis of the

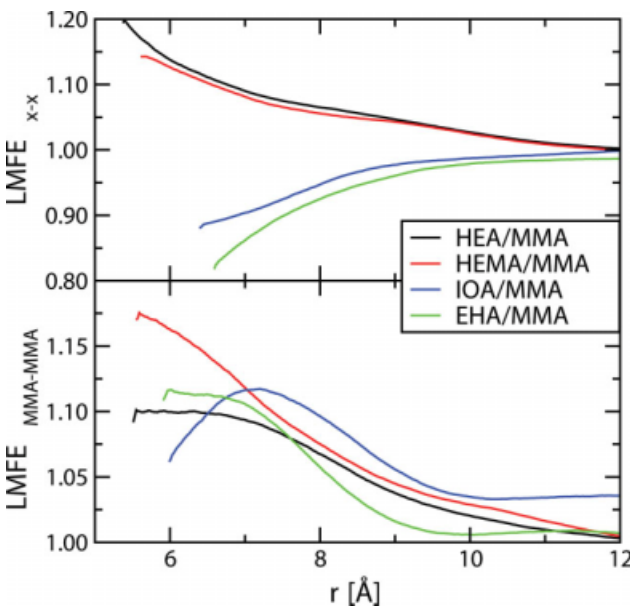

Figure 4 Comparison of the local molfraction enhancement (LMFE) for four binary mixtures with 50/50 bulk molfraction: HEA/MMA (black lines), HEMA/MMA (red lines), EHA/MMA (green lines), and IOA/MMA (blue lines). The top part shows the LMFE of component I being surrounded by other component I molecules (e.g., HEA being surrounded by HEA for the black line), and the bottom part shows the LMFE for MMA being surrounded by MMA (i.e.,component II). [Color figure can be viewed in the online issue, which is available at www.interscience.wiley.com.]

H-bonds formed in the mixture. Using an H-bond criterion based on O—O and O—H distances and the bond angle,[44] one finds that on average each HEA or HEMA molecule forms 0.85 H-bonds in the 50/50 mixture (only a 5% decrease compared with pure HEA or HEMA) and that about 84% of these H-bonds involve a hydroxyl oxygen as acceptor site, whereas the HEA/HEMA or MMA carbonyl oxygen atoms each account for approximately 6% of the H-bonds. Given the large number of competing acceptor sites, the microheterogeneity of these acrylate mixtures is very small compared with mixtures of primary alcohols and *n*-alkanes (e.g., 1-hexanol and *n*-hexane[45,46]). The reason for the depletion in the EHA/EHA and IOA/IOA LMFE is one of size, i.e., the van-der-Waals volumes of these molecules are significantly larger than that of MMA and, hence, the first solvation shell around EHA or IOA is slightly enriched by MMA (or depleted by EHA or IOA).

CONCLUSIONS

Hildebrand solubility parameters for a variety of acrylate and methacrylate esters can be predicted with very good accuracy using the TraPPE-UA force field and less so with the CED method using the Dreiding force field. The TraPPE-UA predictions show a mean unsigned percent error of 2% (or 0.2 Hildebrand units) to the average of multiple literature data and usually fall within the range (typically, about 0.6 Hildebrand units) of the available data. In contrast, the Dreiding force field greatly overpredicts the solubility parameters for every molecule studied in this work, mainly because of its large values for the Hansen polar/electrostatic parameter δ_p, which is about three times larger than that computed with the TraPPE force field.

Correlations based on either the normal boiling point or the refractive index fail to predict the correct dependence of the Hildebrand solubility parameters of acrylate and methacrylate esters on the length of the *n*-alkyl chain, but the boiling-point correlation yields acceptable predictions for short side chains including the hydroxyethyl esters.

The solubility parameter of mixtures of MMA and other nonpolar monomers (EHA and IOA) can be well approximated from knowledge of the cohesive energy and molar volume of the individual components, whereas those for mixtures with HEA and HEMA show small positive deviations from a linear interpolation using the pure compound cohesive energies and molar volumes. Structural analysis demonstrates local mole fraction enhancements of the 2-hydroxyethyl ester compounds for the latter mixtures because the hydroxyl oxygen is the preferred hydrogen-bond acceptor site.

In the absence of experimental solubility parameters or relevant physical property data, such as ΔH_{vap} and densities, solubility parameters can be predicted with high accuracy with the TraPPE force field, and such values are likely to be more accurate than group-additive methods or even calculations from piece-wise experimental data, as all simulated results are indeed determined at the proper temperature and pressure.

References

1. Coleman, M. M.; Serman, C. J.; Bhagwagar, D. E.; Painter, P. C. Polymer 1990, 31, 1187.
2. Paul, D. R.; Barlow, J. W. Polymer 1984, 25, 487.
3. Karst, D.; Yang, Y. J Appl Polym Sci 2005, 96, 416.
4. Hildebrand, J. H.; Scott, R. L. The Solubility of Nonelectrolytes, 3rd ed. Reinhold: New York, 1950.
5. Barton, A. F. M. CRC Handbook of Solubility Parameters and Other Cohesion Parameters. CRC Press: Boca Raton, FL, 1983.
6. Brandrup, J.; Immergut, E. H.; Grulke, E. A.; Abe, A.; Bloch, D. R. Polymer Handbook, 4th ed. Wiley: New York, 1999.
7. Zeng, W.; Du, Y.; Xue, Y.; Frisch, H. L. Solubility Parameters. In: Mark JE, Ed. Physical Properties of Polymers Handbook, 2nd ed. Springer: New York, 2007; Chapter 16.
8. Gardon, J. L. J Paint Technol 1966, 38, 43.
9. Hoy, K. L. J Paint Technol 1970, 42, 76.
10. Barton, A. F. M. Chem Rev 1975, 75, 731.
11. Crowley, J. D.; Teague, G. S.; Lowe, J. W. J Paint Technol 1966, 38, 269.
12. Hansen, C. M. J Paint Technol 1967, 39, 104.
13. Hansen, C. M. Hansen Solubility Parameters: A User's Handbook, 2nd ed. CRC Press: Boca Raton, FL, 2007.
14. Yaws, C. L. Yaws' Handbook of Thermodynamic and Physical Properties of Chemical Compounds. Knovel: Norwich, NY, 2003.
15. Belmares, M.; Blanco, M.; Goddard, W. A.; Ross, R. B.; Caldwell, G.; Chou, S.; Pham, J.; Olafson, P. M.; Thomas, C. J Comput Chem 2004, 25, 1814.
16. Jawalkar, S. S.; Ador, S. G.; Sairam, M.; Nadagouda, N. M.; Aminabhavi, T. M. J Phys Chem B 2005, 109, 15611.
17. Jawalkar, S. S.; Aminabhavi, T. M. Polymers 2006, 47, 8061.
18. Jawalkar, S. S.; Raju, K. V. S. N.; Halligudi, S. B.; Sairam, M.; Aminabhavi, T. M. J Phys Chem B 2007, 111, 2431.
19. Rai, N.; Siepmann, J. I.; Schultz, N. E.; Ross, R. B. J Phys Chem C 2007, 111, 15634.
20. Rai, N.; Wagner, A. J.; Ross, R. B.; Siepmann, J. I. J Chem Theory Comput 2008, 4, 136.
21. Allen, M. P.; Tildesley, D. J. Computer Simulation of Liquids. Oxford UP: New York, 1987.
22. Frenkel, D.; Smit, B. Understanding Molecular Simulation: From Algorithms to Applications, 2nd ed. Academic Press: San Diego, CA, 2002.
23. Martin, M. G.; Siepmann, J. I. J Phys Chem B 1998, 102, 2569.
24. Martin, M. G.; Siepmann, J. I. J Phys Chem B 1999, 103, 4508.
25. Chen, B.; Potoff, J. J.; Siepmann, J. I. J Phys Chem B 2001, 105, 3093.
26. Stubbs, J. M.; Potoff, J. J.; Siepmann, J. I. J Phys Chem B 2004, 108, 17596.
27. Maerzke, K. A.; Schultz, N. E.; Ross, R. B.; Siepmann, J. I. J Phys Chem B 2009, 113, 6415.
28. Mayo, S. L.; Olafson, B. D.; Goddard, W. A. J Phys Chem 1990, 94, 8897.
29. Maitland, G. C.; Rigby, M.; Smith, E. B.; Wakeham, A. Intermolecular Forces: Their Origin and Determination. Pergamon Press: Oxford, 1987.

30. Siepmann, J. I.; Frenkel, D. Mol Phys 1992, 75, 59.
31. Vlugt, T. J. H.; Martin, M. G.; Smit, B.; Siepmann, J. I.; Krishna, R. Mol Phys 1998, 94, 727.
32. Rehberg, C. E.; Fisher, C. H. Ind Eng Chem 1948, 40, 1429.
33. Lide, D. R., editor. CRC Handbook of Chemistry and Physics, 89th ed. CRC Press/Taylor and Francis: Boca Raton, FL, 2009.
34. Koenhen, D.M.; Smolders, C.A. J Appl Polym Sci 1975, 19, 1163.
35. Lawson, D. D.; Ingham, J.D. Estimation of Solubility Parameters from Refractive Index Data. Nature 1969, 223, 614.
36. Askadskii, A. A. Physical Properties of Polymers: Prediction and Control. Gordon and Breach: Amsterdam, 1996.
37. Weast, R. C., editor. CRC Handbook of Chemistry and Physics, 57th ed. CRC Press: Cleveland, OH, 1976–1977.
38. Rehberg, C. E.; Fisher, C. H. J Am Chem Soc 1944, 66, 1203.
39. Rehberg, C. E.; Faucette, W. A.; Fisher, C. H. J Am Chem Soc 1944, 66, 1723.
40. Sigma-Aldrich Company. Aldrich Handbook of Fine Chemicals and Laboratory Equipment. Sigma-Aldrich Company: Milwaukee, WI, 2008.
41. Zhuravlev, N. D.; Martin, M. G.; Siepmann, J. I. Fluid Phase Equil 2002, 202, 307.
42. Pitzer, K. S. J Chem Phys 1939, 7, 583.
43. Becke, A. D. J Chem Phys 1993, 98, 5648; Lee, C.; Yang, W.; Parr, R. G. Phys Rev B 1988, 37, 785; Hehre, W. J.; Radom, L.; Schleyer, P. v. R.; Pople, J. A. Ab initio Molecular Orbital Theory; Wiley: New York, NY, 1986.
44. Stubbs, J. S.; Siepmann J. I. J Am Chem Soc 2006, 127, 4722.
45. Stubbs, J. S.; Siepmann J. I. J Phys Chem B 2002, 106, 3968.
46. Gupta, R. B.; Brinkley, R. L. AIChE J 1998, 44, 207.